



Published in final edited form as:

Nucl Med Biol. 2012 July ; 39(5): 645–651. doi:10.1016/j.nucmedbio.2011.12.001.

Pretargeting vs direct targeting of human betalox5 islet cells subcutaneously implanted in mice using an anti-human islet cell antibody

Guozheng Liu^{1,*}, Shuping Dou¹, Ali Akalin¹, Mary Rusckowski¹, Philip R Streeter², Leonard D. Shultz³, and Dale L Greiner¹

¹University of Massachusetts Medical School, Worcester, MA 01655

²Oregon Health & Science University, Portland, OR 97239

³The Jackson Laboratory, Bar Harbor, ME 06409

Abstract

Introduction—Our previous investigation showed the proof-of-concept of islet cell and islet imaging by pretargeting, however, it is important to know whether the pretargeting strategy was really playing a key role. The improvement by pretargeting over direct targeting is now evaluated in terms of target accumulations and target/non-target (T/NT) ratios.

Methods—Specific binding of an anti-human islet antibody HPi1 to betalox5 human beta cells transplanted subcutaneously in mice was examined against a negative antibody control. Pretargeting by MORF-HPi1 plus ¹¹¹In-labeled cMORF was then compared to direct targeting by ¹¹¹In-labeled HPi1.

Results—HPi1 binding to betalox5 human cells in the transplant was visualized directly by immunofluorescence. Normal organ ¹¹¹In backgrounds by pretargeting were always lower, although target accumulations were similar. The transplant to pancreas and liver ratios were respectively 26 and 10 by pretargeting as compared to 9 and 0.6 by direct targeting.

Conclusions—Pretargeting greatly improves T/NT ratios and, based on the estimated endocrine to exocrine ratio within a pancreas, pretargeting may be approaching the sensitivity required for successful targeting of human islets within a pancreas

Keywords

Pretargeting; Islet cell imaging; T/NT ratios; Anti-human islet antibody

© 2011 Elsevier Inc. All rights reserved.

*Request for reprints: Guozheng Liu, Ph D, Division of Nuclear Medicine, Department of Radiology, University of Massachusetts Medical School, 55 Lake Avenue North, Worcester, MA 01655-0243. Phone: 508-856-1958; Fax: 508-856-6363. guozheng.liu@umassmed.edu.

DISCLOSURE

OHSU has commercially licensed part of the technology disclosed herein (HPi1); P.R.S. is an inventor of this reagent. This potential conflict of interest has been reviewed and managed by OHSU.

Publisher's Disclaimer: This is a PDF file of an unedited manuscript that has been accepted for publication. As a service to our customers we are providing this early version of the manuscript. The manuscript will undergo copyediting, typesetting, and review of the resulting proof before it is published in its final citable form. Please note that during the production process errors may be discovered which could affect the content, and all legal disclaimers that apply to the journal pertain.

INTRODUCTION

For individuals with either type 1 and type 2 diabetes (T1D and T2D), a noninvasive method is greatly needed to measure the islet cell mass in the pancreas or following islet transplantation [1–8]. However, developing such a method has imposed serious challenges to molecular imaging. Islets constitute only about 1–2% of the pancreas mass in healthy individuals and, of these, 65–80% are the insulin-secreting beta cells. Apart from the paucity of beta cells, imaging is particularly difficult due to the proximity of the pancreas to internal organs that form the clearance pathway of radiopharmaceuticals. The interference of surrounding tissues is even more pronounced when attempting to image intraportal islet transplants within the liver. These difficulties will eventually be expressed as low target to non-target (T/NT) ratios, including the conventional target to normal organ ratios (external T/NT ratios) and the target tissue to non-target tissue ratios within the target organ (internal T/NT ratio). Typical examples for the latter include the endocrine/exocrine ratio in pancreas and the islet/liver ratio in liver with islet transplants. While numerous efforts using different agents and different imaging modalities are under investigation [9–14], an effective method that can be translated to the clinic has yet to be reported.

Pretargeting addresses the difficulties in direct targeting of cancer associated with the slow pharmacokinetics of radiolabeled antibody and the high accumulation and prolonged retention of radioactivity in liver and other organs [15–19]. Using an anti-human islet antibody HPi1, we recently provided a proof-of concept that our pretargeting approach using a pair of mutually complementary phosphorodiamidate morpholino oligomers (MORF/cMORF pretargeting) is useful for beta cell imaging [20]. However, it is important to know whether the MORF/cMORF pretargeting really plays an important role in this achievement and whether it will be useful in future human studies. Using this HPi1 antibody again, we now measure the extent to which that MORF/cMORF pretargeting can improve over the direct targeting. Although both subcutaneous islet transplants and subcutaneous betalox5 islet cell transplants are useful models [20], we choose to use the latter in this investigation for its ready availability with less batch to batch variation. In addition, we further confirm the islet binding specificity of HPi1 using a negative antibody control alternative to the negative cell line control used previously [20].

MATERIALS AND METHODS

Cells and Mice

The betalox5 cell line (immortal human beta cells) was a gift from Dr. Pamela Itkin-Ansari (San Diego, CA) [21]. The NOD. Cg-Prkdc^{scid} IL2rg^{tm1Wjl}/SzJ (NSG) mice were obtained from the colony of Dr. Leonard Shultz at The Jackson Laboratory (Bar Harbor, ME) [22]. The CD-1 mice used in the clearance kinetic study were obtained from the Charles River Laboratories (Wilmington, MA). The betalox5 cell line was grown in our laboratories as well as in the UMMS Tissue Culture Core facility. All NSG mice were housed in a pathogen free facility in microisolator cages, given autoclaved food and maintained on acidified autoclaved water medicated with sulfamethoxazole-trimethoprim (Goldline Laboratories, Ft. Lauderdale, FL) on alternate weeks. All animal use was in accordance with the guidelines of the Animal Care and Use Committee of The University of Massachusetts Medical School and The Jackson Laboratory and conformed to the recommendations in the *Guide for the Care and Use of Laboratory Animals* (Institute of Laboratory Animal Resources, National Research Council, National Academy of Sciences, 1996).

Native, MORF-Modified, and ^{111}In -Labeled Antibodies

The mouse anti-human-islet IgG antibody HPi1 was developed in the laboratory of Philip Streeter at Oregon Health & Science University, Portland, OR [23]. After conjugation with an 18-mer MORF, the antibody quality was validated using previously reported procedures [20]. The antibody was also conjugated with the cyclic DTPA dianhydride and labeled with ^{111}In using previously reported procedures [24–26]. The anti-PMSA (prostate membrane specific antigen) IgG antibody 3C6 was obtained from Northwest Biotherapeutics (Bothell, WA) and was also conjugated with MORF in the identical fashion.

Radiolabeled cMORF

The 3'-equivalent terminus amine-derivatized MORF and cMORF with our usual base sequences [27, 28] were obtained from Gene-Tools (Philomath, OR). The cMORF effector was conjugated with the cyclic DTPA dianhydride for ^{111}In labeling [27]. The ^{111}In as InCl_3 and the ^{99}Mo - $^{99\text{m}}\text{Tc}$ generator were obtained from Perkin Elmer Life Science Inc. (Boston, MA, USA). All chemicals were reagent grade and were used without purification.

Cell binding in culture

This experiment was designed to confirm in cell culture the negative binding to the betalox5 cells of the 3C6 antibody selected as a negative control. A total of 18 wells of two 12-well tissue culture plates were seeded with 0.4 million betalox5 cells/well. Two days later the wells were divided into two sets, each with 3 groups (A, B, and C; N=3). The culture medium in each well was replaced with 0.20 mL of culture media containing 30 ng of MORF-HPi1 (average gpm= 0.88) or MORF-3C6 (average gpm 0.50) (group A), 30 ng of native (unconjugated) HPi1 or native 3C6 (group B), or cell culture medium only (group C). All cells were incubated for 1 h at 37°C. The medium was removed and the cells were washed three times with medium. Each well subsequently received 0.20 mL of culture medium containing 0.6 ng $^{99\text{m}}\text{Tc}$ -cMORF. Five minutes later, the medium was removed, the cells were rinsed, and the radioactivity of both the medium and cells was measured in a NaI(Tl) well counter (Cobra II automatic gamma counter, Packard Instrument Company, CT).

Ex vivo tissue staining

The betalox5 transplant model was identical to that used previously [20]. Each NSG mouse was euthanized 4 d after receiving 20 million betalox5 cells subcutaneously in the right flank, the flank was excised and immediately placed in a Nalgene vial (Rochester, NY), embedded in Tissue-Tek OCT compound (Sakura Finetek USA, Inc. Torrance, CA), and frozen by dry ice. The tissue block was sectioned at 5 μm and the slides were fixed in acetone for 5 min at 4 °C. After air drying, 3 slides were treated respectively with HPi1, 3C6, or just buffer at room temperature for 30 min. Sections were washed with PBS and then incubated at room temperature for 30 min with a Cy3-conjugated polyclonal goat anti-mouse antibody (Millipore; Gt X Ms IgG (H+L); catalog #AP124C) diluted 1:100 in PBS containing 5% FBS. The slides were then washed with PBS and were treated with a mounting solution containing hechst before assessment by fluorescence microscopy. H&E staining was performed to confirm presence and location of betalox5 cells within the tissue.

Pharmacokinetics of ^{111}In -cMORF and $^{99\text{m}}\text{Tc}$ -cMORF

To avoid introducing possible label-induced differences, the DTPA bifunctional chelator was used to label both the antibodies and the cMORF effector with ^{111}In . However, optimization of pretargeting parameters (dosages and timing) requires knowledge of the pharmacokinetics of the effectors [29]. Therefore the pharmacokinetics of cMORF after radiolabeling with ^{111}In using DTPA as chelator was compared to that of our routinely

used ^{99m}Tc -cMORF using NHS-MAG₃ as chelator [28]. If the two labeled cMORFs have a similar pharmacokinetic profile, the same pretargeting dosage and timing used previously for ^{99m}Tc -cMORFs could be adopted for ^{111}In -cMORF. Thus, 20 CD-1 mice each received 1 μg (50 μCi) of ^{99m}Tc -cMORF or 1 μg (7 μCi) of ^{111}In -cMORF via a tail vein injection and were divided into 5 groups (N=4) for sacrifice at 10, 30 min, 1, 3, and 6 h. Organs and blood were harvested, weighed, and counted in the NaI(Tl) well counter along with a standard of the injectate for biodistribution determination.

Comparison between direct targeting and pretargeting

As will be shown, the pharmacokinetics of ^{99m}Tc - and ^{111}In -cMORFs were confirmed to be very similar such that the antibody and cMORF dosages and the pretargeting timing could be retained for the current experiment. Each of 16 NSG mice was injected subcutaneously in the right flank with 20 million of betalox5 cells. After 4 d, 8 mice received 30 μg of MORF-HPi1 (average gpm =1.2) followed 2 d later by 4.3 μg (12 μCi) of ^{111}In -cMORF. The remaining group of 8 mice each received 30 μg (13 μCi) of ^{111}In -HPi1. Half of the animals in each group were euthanized at 3 h and the other half at 10 h post radioactivity administration. Except for the accumulation in the target flank that was measured against the contralateral flank as described previously (20), the radioactivity counting and data processing for biodistribution were identical to those performed on the normal mice.

RESULTS

Cell binding in culture

The significantly higher binding of ^{99m}Tc -cMORF to cells treated with MORF-HPi1 compared to cells treated with native HPi1 antibody and to untreated cells is shown in Fig 1A, reproducing the previously observed positive binding of HPi1 to the betalox5 cells [20]. Using a similar approach, Fig 1B shows that the 3C6 antibody does not bind to betalox5 cells, suggesting that the 3C6 antibody can be used as a negative control.

Ex vivo tissue staining

H&E staining (data not shown) indicates that, at 4 d, only the betalox5 cells in the peripheral region of the transplant (about 35% of the target mass) are viable but not the cells in the inner region possibly due to the lack of supporting stroma and/or insufficient blood supply. The betalox5 cells form a compact tumor at the transplant site and are effectively visualized by the nuclear stain Hechst (Fig 2, blue). Immunohistochemical staining of the tissue shows that HPi1 binds to the betalox5 cells in the transplant (Fig 2A) in contrast to the control antibody 3C6 (Fig 2B) that produces weak fluorescence intensity similar to the tissue treated only with the secondary antibody (C).

Pharmacokinetics of ^{111}In -cMORF and ^{99m}Tc -cMORF

Table 1 presents the biodistribution results over 6 h for ^{111}In -cMORF and ^{99m}Tc -cMORF in normal mice, showing rapid whole body clearance for both that is essentially completed in 3 h. While the blood level of ^{111}In -cMORF is slightly lower initially, the area under the blood curve is very similar to that of ^{99m}Tc -cMORF since ^{111}In -cMORF is retained slightly longer in circulation. Since tumor accumulation is proportional to the area under the blood curve [29], when these labeled cMORFs are used as an effector, a similar tumor accumulation may be expected. The kidney accumulation of ^{111}In -cMORF is higher than that of ^{99m}Tc -cMORF but the liver accumulation is lower. Finally ^{111}In -cMORF does not accumulate in the intestines, as observed by us earlier [30].

Comparison between direct targeting and pretargeting

Table 2 compares direct targeting by ^{111}In labeled HPi1 and pretargeting by MORF-HPi1 and ^{111}In -cMORF. While the target accumulations are comparable, the accumulations by direct targeting in normal tissues are many fold higher than accumulations by pretargeting. Accordingly, as shown in Fig. 3, the external (i.e., target to normal organ) T/NT ratios are superior in all organs by pretargeting at both 3 and 10 h. The %ID/g of the betalox5 target is not listed in Table 2, because of the difficulty of accurately removing the small target for weighting free of surrounding tissue. A weight estimate of 40 mg was used in calculating the estimated T/NT ratios in Fig 3. The slight inaccuracy in target weight will not jeopardize the comparison of ratios.

DISCUSSION

This investigation of beta cell targeting again used a mouse model in which human betalox5 cells (an immortal human beta cell line) were implanted subcutaneously in the flank to serve as the target for the anti-human islet cell HPi1 antibody. As was described in the introduction, the targeting of beta cells in the pancreas or transplants is particularly challenging due to the well-recognized factors that contribute to unfavorable T/NT ratios. We have now measured the improvement in T/NT radioactivity ratios in mice by MORF/cMORF pretargeting compared to direct targeting by HPi1. For example, at 10 h, the ratio of the target to liver, spleen, lung, pancreas, and kidney were respectively 16, 10, 5, 3, and 3 fold higher by pretargeting over direct targeting (Fig 3). This suggests that it will be hard to get a discernable image of the target by direct targeting, in contrast to what we observed by pretargeting (20).

Specific binding of HPi1 antibody to the betalox5 cells was validated in our previous studies by use of a negative human cell line. In this study, using the negative control antibody 3C6 from our previous study [31], we confirmed that the HPi1 antibody binds specifically to antigens on the cell membrane in culture. Furthermore, Ex vivo histochemical results using the same antibody control show the specific targeting of this HPi1 antibody with betalox5 cells in the transplant (Fig 2).

Because the HPi1 antibody used in this investigation is specific for human and not mouse islet cells, accumulations of radioactivity in the mouse pancreas in this case is nonspecific. Because 98% of the pancreas is composed of non-target exocrine cells, the accumulations in mouse pancreas in this study may be used as a measure of the nonspecific radioactivity accumulation in future studies with antibodies specific for mouse islet cells. Coupled with the accumulations in the target betalox5 cells of the transplant of this study, these nonspecific pancreas accumulation estimates may be used to roughly estimate the future internal T/NT ratio of pancreas. Assuming an identical beta cell accumulation of 8.8 %ID/g (0.35 %ID/organ/0.04 g) and a pancreas background of 0.25 %ID/g at 10 h from Table 2, the internal T/NT ratio would be about 35. Furthermore, since about two thirds of betalox5 cells in the target were not viable (H&E staining, data not presented), this would raise the estimate to about 100. In addition, because the blood supply to islets in the pancreas [32] may be expected to greatly exceed that to the subcutaneous transplant of this investigation, we anticipate that an internal T/NT ratio greatly in excess of 100 may be expected. Based on the estimate that an internal T/NT ratio of about 1000 may be necessary for imaging [33], our results suggest that MORF/cMORF pretargeting is beginning to approach the sensitivity required for success in islet targeting within an intact pancreas.

CONCLUSION

The beta cell pretargeting approach of this investigation greatly improved the radioactivity accumulation ratios of target to normal organs including the pancreas over the conventional direct targeting. These results suggest that the pretargeting strategy using the anti-human islet cell antibody should also be more sensitive than direct targeting for imaging human islets within the pancreas or following islet transplantation in humans.

Acknowledgments

This work was supported by grants DK82894, DK310 94199, CA94994, and DK89572 and a DERC center grant DK32520 from the National Institutes of Health. We also acknowledge support from The Helmsley Foundation and The Juvenile Diabetes Research Foundation. We thank Dr Donald J Hnatowich from University of Massachusetts Medical School, Worcester, MA for his help in discussion of the research and preparation of the manuscript, Dr. Pamela Itkin-Ansari from the University of California San Diego and Sanford-Burnham Medical Research Institute, San Diego, CA for her generous gift of the betalox5 cell line and Maria Grompe and Yong-Ping Zhong of the OHSU monoclonal antibody shared resource for their support in antibody preparation and immunofluorescence analyses.

References

1. Paty BW, Bonner-Weir S, Laughlin MR, McEwan AJ, Shapiro AM. Toward development of imaging modalities for islets after transplantation: insights from the National Institutes of Health Workshop on Beta Cell Imaging. *Transplantation*. 2004; 77:1133–1137. [PubMed: 15114073]
2. Souza F, Freeby M, Hultman K, et al. Current progress in noninvasive imaging of beta cell mass of the endocrine pancreas. *Curr Med Chem*. 2006; 13:2761–2773. [PubMed: 17073627]
3. Moore A. Advances in beta-cell imaging. *Eur J Radiol*. 2009; 70:254–257. [PubMed: 19261414]
4. Malaisse WJ, Louchami K, Sener A. Noninvasive imaging of pancreatic beta cells. *Nat Rev Endocrinol*. 2009; 5:394–400. [PubMed: 19468290]
5. Brom M, Andrazojc K, Oyen WJ, Boerman OC, Gotthardt M. Development of radiotracers for the determination of the beta-cell mass in vivo. *Curr Pharm Des*. 2010; 16:1561–1567. [PubMed: 20146667]
6. Martinic MM, von Herrath MG. Real-time imaging of the pancreas during development of diabetes. *Immunol Rev*. 2008; 221:200–213. [PubMed: 18275484]
7. Villiger M, Goulley J, Martin-Williams EJ, Grapin-Botton A, Lasser T. Towards high resolution optical imaging of beta cells in vivo. *Curr Pharm Des*. 2010; 16:1595–1608. [PubMed: 20146662]
8. Medarova Z, Moore A. MRI as a tool to monitor islet transplantation. *Nat Rev Endocrinol*. 2009; 5:444–452. [PubMed: 19546863]
9. Evgenov NV, Medarova Z, Dai G, Bonner-Weir S, Moore A. In vivo imaging of islet transplantation. *Nat Med*. 2006; 12:44–48. [PubMed: 16397563]
10. Antkowiak PF, Tersey SA, Carter JD, et al. Noninvasive assessment of pancreatic beta-cell function in vivo with manganese-enhanced magnetic resonance imaging. *Am J Physiol*. 2009; 296:E573–578.
11. Goland R, Freeby M, Parsey R, et al. ^{11}C -dihydrotrabenazine PET of the pancreas in subjects with long-standing type 1 diabetes and in healthy controls. *J Nucl Med*. 2009; 50:382–389. [PubMed: 19223416]
12. Kung MP, Hou C, Lieberman BP, et al. In vivo imaging of beta-cell mass in rats using ^{18}F -FP-(+)-DTBZ: a potential PET ligand for studying diabetes mellitus. *J Nucl Med*. 2008; 49:1171–1176. [PubMed: 18552132]
13. Wild D, Behe M, Wicki A, et al. [Lys40(Ahx-DTPA- ^{111}In)NH $_2$]exendin-4, a very promising ligand for glucagon-like peptide-1 (GLP-1) receptor targeting. *J Nucl Med*. 2006; 47:2025–2033. [PubMed: 17138746]
14. Körner M, Stöckli M, Waser B, Reubi JC. GLP-1 receptor expression in human tumors and human normal tissues: potential for in vivo targeting. *J Nucl Med*. 2007; 48:736–743. [PubMed: 17475961]

15. Karacay H, Brard PY, Sharkey RM, et al. Therapeutic advantage of pretargeted radioimmunotherapy using a recombinant bispecific antibody in a human colon cancer xenograft. *Clin Cancer Res*. 2005; 11:7879–7885. [PubMed: 16278412]
16. Sharkey RM, Cardillo TM, Rossi EA, et al. Signal amplification in molecular imaging by pretargeting a multivalent, bispecific antibody. *Nat Med*. 2005; 11:1250–1255. [PubMed: 16258537]
17. Pagel JM, Hedin N, Subbiah K, et al. Comparison of anti-CD20 and anti-CD45 antibodies for conventional and pretargeted radioimmunotherapy of B-cell lymphomas. *Blood*. 2003; 101:2340–2348. [PubMed: 12446461]
18. Subbiah K, Hamlin DK, Pagel JM, et al. Comparison of immunoscintigraphy, efficacy, and toxicity of conventional and pretargeted radioimmunotherapy in CD20-expressing human lymphoma xenografts. *J Nucl Med*. 2003; 44:437–445. [PubMed: 12621012]
19. Magnani P, Paganelli G, Modorati G, et al. Quantitative comparison of direct antibody labeling and tumor pretargeting in uveal melanoma. *J Nucl Med*. 1996; 37:967–971. [PubMed: 8683323]
20. Liu G, Dou S, Cheng D, et al. Human islet cell MORF/cMORF pretargeting in a xenogeneic murine transplant model. *Mol Pharm*. 2011; 8:767–773. [PubMed: 21361360]
21. de la Tour D, Halvorsen T, Demeterco C, et al. Beta-cell differentiation from a human pancreatic cell line in vitro and in vivo. *Mol Endocrinol*. 2001; 15:476–483. [PubMed: 11222748]
22. Shultz LD, Lyons BL, Burzenski LM, et al. Human lymphoid and myeloid cell development in NOD/LtSz-scid IL2 γ ^{null} mice engrafted with mobilized human hematopoietic stem cell. *J Immunol*. 2005; 174:6477–6489. [PubMed: 15879151]
23. Dorrell C, Abraham SL, Lanxon-Cookson KM, Canaday PS, Streeter PR, Grompe M. Isolation of major pancreatic cell types and long-term culture-initiating cells using novel human surface markers. *Stem Cell Res*. 2008; 1:183–194. [PubMed: 19383399]
24. Hnatowich DJ, Layne WW, Childs RL, et al. Radioactive labeling of antibody: a simple and efficient method. *Science*. 1983; 220:613–615. [PubMed: 6836304]
25. Liu G, Liu C, Zhang S, et al. Investigations of technetium-99m morpholino pretargeting in mice. *Nucl Med Commun*. 2003; 24:697–705. [PubMed: 12766607]
26. Liu G, Dou S, Pretorius PH, Liu X, Rusckowski M, Hnatowich DJ. Pretargeting CWR22 prostate tumor in mice with MORF-B72.3 antibody and radiolabeled cMORF. *Eur J Nucl Med Mol Imaging*. 2008; 35:272–280. [PubMed: 17909792]
27. Liu G, Dou S, Rusckowski M, Greiner D, Hnatowich DJ. Preparation of ¹¹¹In-DTPA morpholino oligomer for low abdominal accumulation. *Appl Radiat Isot*. 2010; 68:1709–1714. [PubMed: 20359901]
28. Liu G, Dou S, He J, et al. Radiolabeling of MAG₃-morpholino oligomers with ¹⁸⁸Re at high labeling efficiency and specific radioactivity for tumor pretargeting. *Appl Radiat Isot*. 2006; 64:971–978. [PubMed: 16730997]
29. Liu G, Hnatowich DJ. A semiempirical model of tumor pretargeting. *Biocojug Chem*. 2008; 19:2095–2104.
30. Liu G, Cheng D, Dou S, et al. Replacing ^{99m}Tc with ¹¹¹In improves MORF/cMORF pretargeting by reducing intestinal accumulation. *Mol Image Biol*. 2009; 11:303–307.
31. Liu G, Dou S, Yin D, et al. A novel pretargeting method for measuring antibody internalization in tumor cells. *Cancer Biother Radiopharm*. 2007; 22:33–39. [PubMed: 17461727]
32. Nyman LR, Wells KS, Head WS, et al. Real-time, multidimensional in vivo imaging used to investigate blood flow in mouse pancreatic islets. *J Clin Invest*. 2008; 118:3790–3797. [PubMed: 18846254]
33. Sweet IR, Cook DL, Lernmark A, Greenbaum CJ, Krohn KA. Non-invasive imaging of beta cell mass: a quantitative analysis. *Diabetes Technol Ther*. 2004; 6:652–659. [PubMed: 15628819]

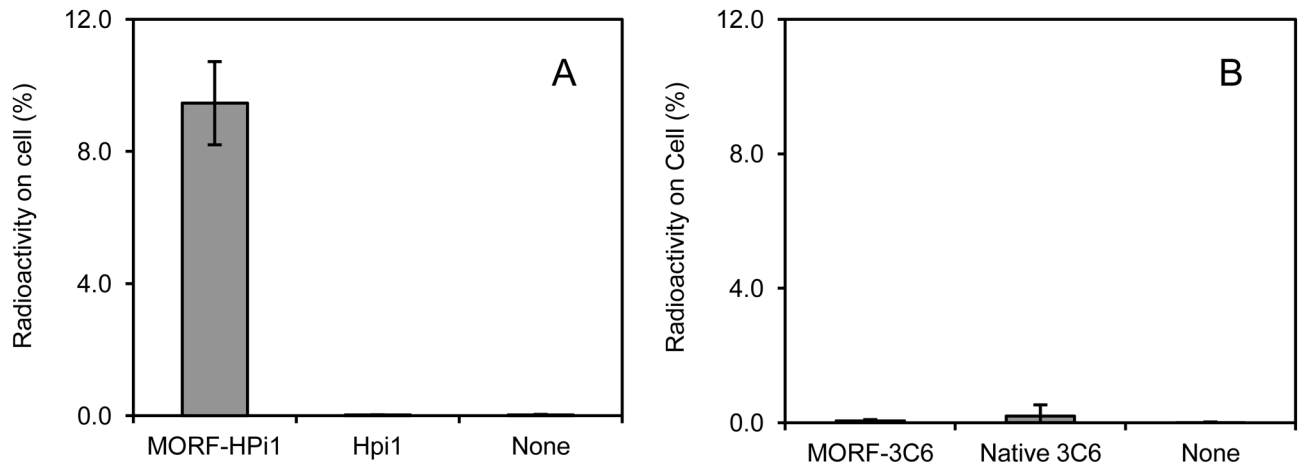


Fig 1.
(A) Accumulations of ^{99m}Tc -cMORF on betaloX5 cells treated with MORF-HPi1, native HPi1, and cells untreated (B) Accumulations on the same cells after treatment with the control 3C6 substitutes.

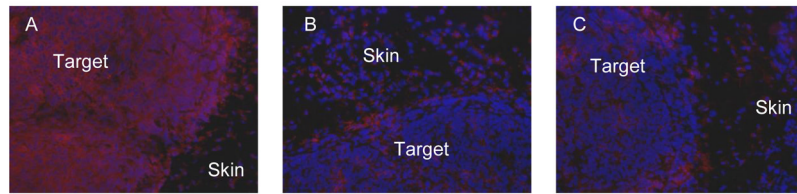


Fig 2.

(A) HPI1 and (B) 3C6 immunohistochemically stained tissue sections compared to (C) the negative control (treated with only the secondary Cy3-conjugated antibody) along with nuclear staining with Hechst (blue). The strong staining of the HPI1-treated section (Cy3; red) in contrast to the 3C6-treated section demonstrates the specific binding of this antibody to the betax5 cells in the transplant. Magnification: 200X.

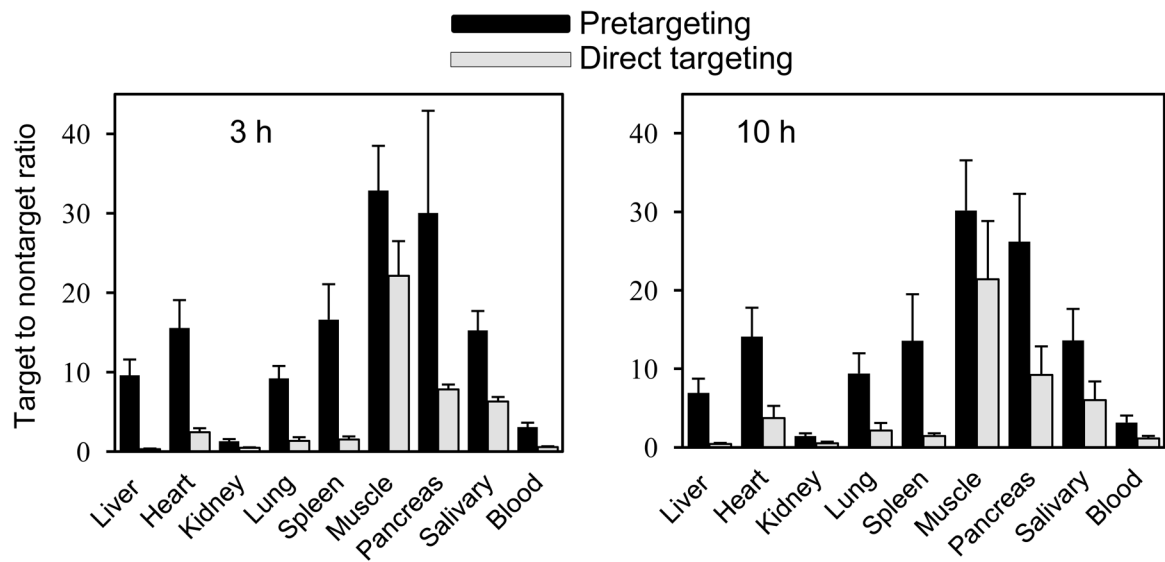


Fig 3.

Histograms presenting the target to non-target ratios for pretargeting using MORF-HPi1 and ^{111}In labeled cMORF and for direct targeting using ^{111}In labeled HPi1. Between pretargeting and direct targeting, $P < 0.05$ for all organs except for muscle at 10 h ($P = 0.06$)

Table 1

Biodistribution of ^{111}In -cMORF and $^{99\text{m}}\text{Tc}$ -cMORF in normal CD-1 mice

%ID/g	^{111}In -cMORF					$^{99\text{m}}\text{Tc}$ -cMORF				
	10min	30 min	1 h	3h	6h	10min	30 min	1 h	3h	6h
Liver	0.51±0.05	0.31±0.04	0.22±0.02	0.23±0.06	0.23±0.02	1.07±0.09	0.76±0.13	0.45±0.05	0.38±0.04	0.44±0.05
Heart	0.79±0.04	0.30±0.03	0.15±0.02	0.10±0.02	0.09±0.01	1.17±0.08	0.53±0.17	0.15±0.01	0.06±0.01	0.05±0.00
Kidney	11.4±4.5	7.30±1.28	5.51±0.68	5.37±0.42	4.27±0.73	4.76±0.81	3.73±0.19	2.43±0.14	2.15±0.26	1.93±0.06
Lung	1.29±0.14	0.47±0.08	0.22±0.03	0.14±0.02	0.13±0.04	2.33±0.40	1.09±0.19	0.38±0.07	0.20±0.05	0.14±0.03
Spleen	0.39±0.03	0.19±0.02	0.12±0.04	0.12±0.02	0.12±0.02	0.70±0.02	0.44±0.07	0.22±0.02	0.14±0.02	0.18±0.05
Muscle	0.69±0.06	0.26±0.05	0.12±0.01	0.08±0.01	0.08±0.01	1.09±0.08	0.42±0.14	0.12±0.02	0.04±0.01	0.04±0.01
Pancreas	0.85±0.06	0.41±0.07	0.19±0.03	0.12±0.01	0.11±0.01	1.25±0.17	0.74±0.17	0.26±0.02	0.07±0.02	0.06±0.01
Salivary	0.92±0.14	0.31±0.05	0.16±0.03	0.15±0.01	0.15±0.02	1.12±0.23	0.55±0.14	0.16±0.01	0.08±0.02	0.08±0.01
Blood	3.05±0.24	1.03±0.12	0.43±0.12	0.22±0.05	0.14±0.02	4.24±0.29	1.64±0.52	0.34±0.04	0.04±0.00	0.02±0.00
%ID/organ										
Stomach	0.25±0.03	0.16±0.05	0.08±0.02	0.06±0.01	0.03±0.00	0.38±0.06	0.17±0.05	0.08±0.02	0.07±0.01	0.06±0.05
Sm. Int.	0.78±0.09	0.39±0.09	0.19±0.02	0.17±0.02	0.14±0.02	1.56±0.26	1.00±0.18	0.55±0.03	0.12±0.03	0.09±0.04
L.g. Int.	0.38±0.05	0.16±0.02	0.06±0.01	0.10±0.01	0.14±0.04	0.64±0.17	0.23±0.07	0.09±0.01	0.52±0.08	0.41±0.15

Table 2

Biodistribution of ^{111}In labeled HPi1 in the NSG mouse model bearing betalox5 transplant (direct targeting) and biodistribution of ^{111}In -cMORF in the same NSG model but pretargeted with MORF-HPi1 (pretargeting). %ID/g and %ID/organ \pm one s.d.

Organ	3 h		10 h	
	Direct targeting	Pretargeting	Direct targeting	Pretargeting
%ID/g				
Liver	23.5 \pm 2.1	0.94 \pm 0.15	22.6 \pm 2.1	0.93 \pm 0.15
Heart	3.21 \pm 0.42	0.60 \pm 0.10	2.55 \pm 0.40	0.46 \pm 0.10
Kidney	16.4 \pm 1.6	6.74 \pm 1.14	17.8 \pm 2.1	4.44 \pm 0.62
Lung	5.84 \pm 1.35	0.93 \pm 0.13	4.60 \pm 0.70	0.68 \pm 0.09
Spleen	5.06 \pm 1.00	0.54 \pm 0.10	6.62 \pm 1.84	0.50 \pm 0.13
Muscle	0.35 \pm 0.02	0.25 \pm 0.04	0.44 \pm 0.04	0.21 \pm 0.05
Pancreas	0.97 \pm 0.10	0.34 \pm 0.15	1.03 \pm 0.12	0.25 \pm 0.05
Salivary	1.20 \pm 0.11	0.60 \pm 0.07	1.57 \pm 0.09	0.48 \pm 0.10
Blood	13.4 \pm 0.9	2.93 \pm 0.38	8.22 \pm 0.85	2.03 \pm 0.25
%ID/organ				
Stomach	0.47 \pm 0.12	0.13 \pm 0.02	0.38 \pm 0.02	0.09 \pm 0.01
Sm. Int.	1.81 \pm 0.10	0.41 \pm 0.07	1.64 \pm 0.17	0.31 \pm 0.02
Lg. Int.	0.77 \pm 0.06	0.31 \pm 0.09	0.12 \pm 0.19	0.38 \pm 0.18
Target	0.30\pm0.04	0.35\pm0.02	0.37\pm0.13	0.26\pm0.09